Two New Supramolecular Compounds that Involve Trans-1,2-bis(4-pyridyl)ethylene (bpe), Barbituric Acid and Fe(II) ions

Humberto C. Garcia, Renata Diniz and Luiz Fernando C. de Oliveira[*]

Núcleo de Espectroscopia e Estrutura Molecular, Departamento de Química, Universidade Federal de Juiz de Fora, Campus Universitário s/n, Martelos, Juiz de Fora, MG, 36036-900, Brazil

Abstract: In this study, the synthesis, spectroscopic properties (infrared and Raman) and crystal structures of two new compounds named $(H_2bpe)B_2 \cdot 2H_2O$ (**1**) and $[Fe(bpe)(H_2O)_4]B_2 \cdot 4H_2O$ (**2**) have been reported, where bpe is *trans*-1,2-bis(4-pyridil)-ethylene, H_2bpe is protonated bpe and B^- is the barbiturate anion. For both complexes, we observed the presence of supramolecular interactions, such as electrostatic, hydrogen bonding and π-stacking interactions. Compound **1** crystallised in a triclinic system with the space group *P-1*, which was generated by cationic and anionic units formed by protonated bpe, the barbiturate anion and water molecules. These molecules interacted through weak intermolecular interactions and were responsible for the crystalline stability of the synthesised compounds. For compound **2**, an orthorhombic crystal system was observed with a P*bcn* space group. In this crystal, the metallic site adopted a distorted octahedral geometry that was coordinated by two pyridine nitrogen atoms and four oxygen atoms from coordinated water molecules. The three-dimensional arrangement of the structure consisted of one covalent one-dimensional linear cationic $[Fe(bpe)(H_2O)_4]^{2+}$ chain, which interacts by forming hydrogen-bonding, π-stacking and electrostatic interactions with barbiturate anions and water molecules that were trapped in the crystal. The vibrational spectra of the two compounds were very similar despite the different crystalline arrangements that were adopted by the two structures. In the infrared spectra, two intense bands at 1684 and 1630 cm^{-1} were observed and assigned to the CO stretching (νCO) of the barbiturate anion and νC=C of the bpe ligand, respectively. In the Raman spectra of the compounds, the most important bands were attributed to the bpe ligand at 1629 and 1006 cm^{-1}, which were assigned to the νC=C and νring, respectively. The presence of the barbiturate anion was confirmed by the presence of a band of low intensity located at 680 cm^{-1} and was assigned as the ring-breathing mode.

INTRODUCTION

The construction of supramolecular arrays through building blocks has developed into a central theme of supramolecular chemistry [1, 2]. Many novel supramolecular complexes have been produced through organic blocks and/or metallic centres to generate expanding systems in one-, two- and three-dimensions [3, 4]. The main purpose of research in this area is the strategic construction of specific architectures as well as a more complete understanding of the connection between the structure and the physical-chemical properties [5]. These types of studies are important for scientific vision and technology and have several applications in optical, electronic, and catalytic processes as well as magnetic properties [6-8].

The investigation of pyrimidine systems has become a focus for several research groups due to their function in biological environments as hypnotic drugs of the nervous system [9] and recently, as building blocks for generating supramolecular systems through weak noncovalent interactions [10]. In this context, barbituric acid has been determined to be a new supramolecular building block because the presence of a pyrimidine ring in its structure favours π-stacking and C-H$\cdots\pi$ type interactions as well as the presence of three carbonyl and two imino groups that can act as hydrogen bond acceptors and donors, respectively. Barbituric acid is a weak acid (pK_a= 3.99) [11] due to the ability of the CH_2 group to lose one of its hydrogen atoms, which provides extra stabilisation to this species by resonance delocalisation [12] and is shown in Fig. (**1**). Barbituric acid and the barbiturates, including the thiobarbiturate anion and violuric acid, possess hydrogen bond donor and acceptor groups, which may make them suitable for crystal engineering materials with specific or programmed properties. In addition, there are already known barbituric acid derivatives that exhibit NLO properties [13, 14].

Another well-known nitrogen ligand in supramolecular chemistry used in this study is *trans*-1,2-bis(4-pyridyl)ethylene (bpe) and is mainly used for its spectroscopic characteristics and properties, such as its catalytic, optic and magnetic properties when combined with other building blocks and metal ions [15, 16]. Bpe can act as a rigid organic ligand or as a bridge between two metallic sites. The protonation of one or two of the nitrogen atoms of

*Address correspondence to this author at the Núcleo de Espectroscopia e Estrutura Molecular, Departamento de Química, Universidade Federal de Juiz de Fora, Campus Universitário s/n, Martelos, Juiz de Fora, MG, 36036-900, Brazil; Tel: +55 (32) 3229-3310; Fax: +55 (32) 3229-3310; E-mail: luiz.oliveira@ufjf.edu.br
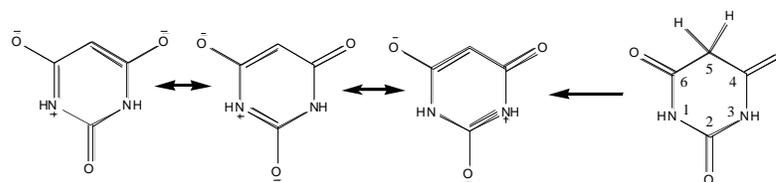
Fig. (1). The molecular structure of barbituric acid, barbiturate anion and the resonance forms.

the pyridyl rings in the molecule is also possible when in acidic media, which expands the possibility for the formation of new structures that involve such systems. Another important feature is their ability to form supramolecular polymer system through the C-H···π type and π-stacking interactions, which generates a stable crystalline arrangement in one-, two- and three-dimensions [17].

In the present work, the synthesis, crystal structure and vibrational spectroscopic analysis (infrared and Raman) of two new supramolecular complexes that involve barbituric acid, bpe and iron (II) ions are described. The objective of this study was to understand the role of each one of the building blocks by relating the spectra and crystal structure of the supramolecular compounds that were obtained.

EXPERIMENTAL SECTION

Chemicals and Reagents

All chemicals used in this study were used as purchased without further purification: barbituric acid ($C_4H_4N_2O_3$, 99.0%, Merck), *trans*-1,2-bis(4-pyridil)-ethylene (bpe) (98.0%, Sigma Aldrich), $ZnSO_4 \cdot 7H_2O$ (99.0%, Vetec) and $FeSO_4 \cdot 7H_2O$ (99.5%, Sigma Aldrich).

Synthesis

The synthesis was similar for both complexes; in general, the compounds were prepared as follows: 15 mL of an aqueous solution that contained 70 mg (0.54 mmol) of barbituric acid (HB) was mixed with 10 mL of an ethanolic solution that contained 50 mg (0.27 mmol) of bpe, which led to a homogenous mixture that was yellow in colour. This solution was added to 5 mL of an aqueous solution that contained 0.27 mmol of a metallic ion solution. After all reagents were mixed, the formation of a precipitate was observed, and the system was stirred and heated to 60°C for 15 minutes, which resulted in the complete solubilisation of the reagents and the formation of a homogeneous mixture that was brown or orange in colour for the zinc and iron salts, respectively. After a few days, suitable single crystals were obtained and separated by filtration. The crystals were analysed by vibrational spectroscopy, thermogravimetric analysis and X-ray diffraction techniques. It is important to note that the only difference between the two compounds was the presence of the metallic ion. The synthesis of compound 1 should have contained a zinc(II) ion; however, the metal was not able to participate in the structure, and only the barbiturate ion and bpe are responsible for the crystalline structure. Elemental analysis: $(H_2bpe)B_2 \cdot 2H_2O$ **(1)** (brown crystals, yield = 56%): Calcd.: C, 50.63%; H, 4.67%; N, 17.71%; Observed: C, 50.41%; H, 4.34%; N, 16.67%. $[Fe(bpe)(H_2O)_4]B_2 \cdot 4H_2O$ **(2)** (orange crystals, yield = 43%): Calcd.: C, 37.75%; H, 5.07%; N, 13.21%; Observed: C, 37.91%; H, 5.29%; N, 12.95%.

PHYSICAL MEASUREMENTS

Thermogravimetric measurements (TG/DTA) were performed using a Shimadzu TG-60 with a thermo balance. Samples were heated at a rate of 10°C min^{-1} from room temperature to 900°C in dynamic nitrogen atmosphere at a flow rate of 100 mL min^{-1}. Infrared spectra were obtained using a Bomem MB-102 spectrometer fitted with a CsI beam splitter with the samples dispersed on KBr disks, and the spectral resolution was acquired at 4 cm^{-1}. Good signal-to-noise ratios were obtained from the accumulation of 128 spectral scans. Fourier-transform Raman spectroscopy was performed using a Bruker RFS 100 instrument with an Nd^{3+}/YAG laser operating at 1064 nm in the near-infrared region and a CCD detector that was cooled with liquid N_2. Good signal-to-noise ratios were obtained from 2000 scans that were accumulated over a period of 30 min with a spectral resolution of 4 cm^{-1}. All spectra were obtained at least twice to show reproducibility, and there were no changes in the band positions or intensities observed. Single crystal X-ray data were collected using an Oxford GEMINI A Ultra diffractometer with MoKα (λ = 0.71073 Å) at room temperature (298K) for compound **(1)** and CuKα (λ = 1.542 Å) at 120K for compound **(2)**. Data collection, reduction and cell refinement were performed by CrysAlis RED, Oxford diffraction Ltda, Version 1.171.32.38 [18]. The structures were determined and refined using SHELXL-97 [19]. The empirical isotropic extinction parameter x was refined according to the method previously described by Larson [20], and a Multiscan absorption correction was applied [21]. The structures were drawn by ORTEP-3 for Windows [22] and Mercury [23] programs. CCDC 790186 and 790187 contained the supplementary crystallographic data for compounds **1** and **2**, respectively. These data can be obtained free of charge at http://www.ccdc.cam.ac.uk or from the Cambridge Crystallographic Data Centre, 12 Union Road, Cambridge CB2 IEZ, UK [Fax: (internat.) 1 44-1223/336-033; E-mail: deposit@ccdc.cam.ac.uk].

RESULTS AND DISCUSSION

It is important to note that the difference between the two compounds investigated was that one only contained the barbiturate ion and bpe; however, this crystal was produced from a solution that contained zinc (II) ions, which were not likely to be part of the supramolecular structure. The results of the thermogravimetric analysis showed important and conclusive information in terms of the previous distinction between complexes **1** and **2**. The thermogravimetric curves are shown in the supplementary materials. The thermogravimetric analysis of $(H_2bpe)B_2 \cdot 2H_2O$ **(1)** shows an initial mass loss at 165.5°C, which was attributed to the loss of two water molecules (calculated/experimental: 7.59%/7.70%) by the structure. There were three other weight loss steps that

Table 1.   Crystal Data from the Complexes of (H₂bpe)B₂·2H₂O (1) and [Fe(bpe)(H₂O)₄]B₂·4H₂O (2)

Compound	(H$_2$bpe)B$_2$·2H$_2$O (1)	[Fe(bpe)(H$_2$O)$_4$]B$_2$·4H$_2$O (2)
Formula	C$_{20}$H$_{22}$N$_6$O$_8$	C$_{20}$H$_{32}$FeN$_6$O$_{14}$
Formula weight/g mol^{-1}	474.44	636.37
Crystal system	Triclinic	Orthorhombic
Space group	*P-1*	*Pbcn*
a/Å	8.265(2)	10.255(2)
b/Å	8.338(2)	14.036(3)
c/Å	8.523(2)	18.787(4)
α	111.71(2)	90.00
β	103.70(2)	90.00
γ	94.69(2)	90.00
V/Å^3	520.75(2)	2704.2 (10)
Z	1	4
Crystal size/mm	0.09 X 0.26 X 0.46	0.09 X 0.17 X 0.17
D$_{calc}$/g cm^{-3}	1.513	1.563
μ(Mo Kα)/cm^{-1}	0.119	5.194
Transmission factors (min/max)	0.80754/1.0000	0.8168/1.0000
Reflections measured/unique	58102/2133	5728/2176
Observed reflections [F$_o^2$>2σ(F$_o^2$)]	1758	1759
N°. of parameters refined	183	224
R[F$_o$>2σ(F$_o$)]	0.0343	0.0326
wR[F$_o$2>2σ(F$_o$)^2]	0.1090	0.0966
S	1.063	1.077
RMS peak/	0.040	0.058

were observed with this experiment, which were attributed to the release of two barbiturate anions and the protonated bpe ligand. The inexistence of residue at 900°C suggests the absence of the zinc (II) ion in the formation of the crystalline complex and the complete thermal decomposition of the analysed organic material. For the [Fe(bpe)(H₂O)₄]B₂·4H₂O (**2**) complex, the thermogravimetric curves show that the first weight loss occurred at 182.5°C, which corresponded to the removal of four water molecules (calcd./exp.: 11.4%/11.6%) of hydration. A second weight loss was observed at 243.4°C and was attributed to the loss of four other coordination water molecules (calcd./exp.: 12.5%/12.3%). The other two weight-loss events that were observed were attributed to the exit or decomposition of the barbiturate anion and the bpe ligand, and the final residue was identified as FeO (calcd./exp.: 11.0%/11.1%). Through thermogravimetric measurements, we observed an initial loss of mass that occurred at high temperatures for both complexes, which suggests a strong interaction of water molecules within the crystal lattice by means of supramolecular interactions, such as hydrogen bonds, which are very common for these types of compounds.

The structural arrangement of both compounds was determined by X-ray single crystal analysis; compound **1** crystallised in a triclinic system, which presented a *P-1* space group, while compound **2** crystallised in an orthorhombic system with a *Pbcn* space group. The crystallographic data, main geometrical parameters and hydrogen interactions for both compounds are presented in Tables **1** and **2**, respectively.

Fig. (**2**) shows the repeating unit for compound **1**, which was formed by the diprotonated bpe cation through the nitrogen atoms of the pyridyl rings. The cationic unity was neutralised by two barbiturate anions, which interacted with each other by hydrogen bonds, and this interaction was classified as a head to tail interaction. The NH group of one barbiturate ion acts as an H-donor, which interacts with the H-acceptor carbonyl group of the other barbiturate. These hydrogen bonds present average O3···N2 bond lengths of 2.876 (2) Å, which is classified as a moderate to weak interaction due to the average distance [24-26]. The presence of anionic and cationic species in the solid structure was explained by a simple acid-basic reaction between the building blocks used in the process. Two molecules of water are present in the crystals. Initially, this process contained Zn (II) ions, which were not able to be part of the supramolecular structure. Fig. (**3**) shows the two-dimensional arrangement for compound **1** along the *bc* plane, and the hydrogen bonds between the two barbiturate anions and a protonated bpe ligand give rise to extended one-dimensional linear chains. An interesting supramolecular arrangement can also be observed for the hydrogen interactions between two barbiturate anions of adjacent one-dimensional linear chains, which gave rise to sheets that contained cavities. These cavities were classified as $N_1 = C(23)R_8^8(51)$ and $N_2 = R_2^2(8)$, where C and R refer to the hydrogen bonds that are present in the linear chains and rings, respectively. The numbers of donors (d) and acceptors

Table 2. **Selected Geometrical Parameters and Hydrogen Interactions of the (H₂bpe)B₂·2H₂O (1) and [Fe(bpe)(H₂O)₄]B₂·4H₂O (2) Complexes**

Bond distance/Å	(H₂bpe)B₂·2H₂O (1)	Bond distance/Å	[Fe(bpe)(H₂O)₄]B₂·4H₂O (2)
O2–C11	1.263(2)	Fe1–O7	2.103(2)
O3–C9	1.232(2)	Fe1–O6	2.091(2)
N2–C9	1.367(2)	Fe1–N3	2.230(2)
N2–C7	1.386(2)	N2–C7	1.386(3)
N1–C9	1.363(2)	N1–C9	1.352(3)
N1–C11	1.389(2)	N1–C11	1.386(3)
O1–C7	1.261(1)	O1–C7	1.273(2)
N3–C4	1.334(2)	N3–C4	1.341(3)
N3–C2	1.342(2)	N3–C2	1.350(3)
C6–C1	1.394(2)	C6–C1	1.399(3)
C6–C5	1.395(2)	C6–C5	1.399(3)
C6–C13	1.470(2)	C6–C13	1.465(3)
C4–C5	1.376(2)	C4–C5	1.378(3)
C1–C2	1.365(2)	C1–C2	1.377(3)
C13–C13	1.332(2)	C13–C13	1.336(6)
Average of bond angles/°		Average of bond angles/°	
C9 – N2 – C7	124.4(1)	O6–Fe1–O6	180.00(9)
C9 – N1 – C11	124.5(2)	O6–Fe–O7	89.95(7)
O1 – C7 – N2	117.5(1)	O6–Fe1–N3	94.44(6)
N2 – C7 – C12	117.3(1)	O7–Fe1–N3	88.14(6)
N1 – C9 – N2	115.5(1)	N3–Fe1–N3	180.00(6)
N3 – C4 – C5	119.7(1)	N3–C4–C5	123.9(2)
N3 – C2 – C1	120.41(1)	N3–C2–C1	123.8(2)
Hydrogen bond		Hydrogen bond	
D⋯A/Å		D⋯A/Å	
N1⋯O2	2.794(1)	N1⋯O3	2.846(2)
N2⋯O3	2.876(2)	N2⋯O1	2.804(2)
N3⋯O1	2.635(1)	O4⋯O3	2.784(2)
O4⋯O1	2.782(2)	O4⋯O2	2.819(2)
O4⋯O2	2.876(2)	O5⋯O2	2.775(2)
		O6⋯O2	2.770(2)
		O7⋯O4	2.681(3)
D–H⋯A/°		D–H⋯A/°	
N1–H1N⋯O2	173.5(2)	N1–H1N⋯O3	176.00
N2–H2N⋯O3	176.0(2)	O4–H4A⋯O3	166(3)
N3–H3N⋯O1	161.4(2)	O7–H7A⋯O4	165(3)

(a) used in each motif were assigned as subscripts and super-scripts, respectively, and the size or degree of the motif (corresponding to the number of atoms in the repeat units) is indicated in the parentheses [27,28]. Other supramolecular interactions occur between two consecutive barbiturate anions of different linear chains with the appearance of a zigzag chain that was generated by hydrogen bonds and extended along the *c*-axis. The two-dimensional array displayed in Fig. (**3**) interacts by hydrogen bonding with water molecules that are trapped in the crystal and are present in the structure along the *a*-crystallographic axis with other two-dimensional layers, which appear slightly shifted from the previous layers and give rise to a 3-D supramolecular arrangement. This 3-D array is responsible for the stability of the crystalline lattice of compound **1** because, in this type of structure, the centroid-centroid distance between the adjacent rings of the barbiturate anion and the pyridyl ring was larger than 3.80 Å, or more precisely 4.33 Å, which indicates that there was no π-stacking interaction between the aromatic rings in these compounds [29].
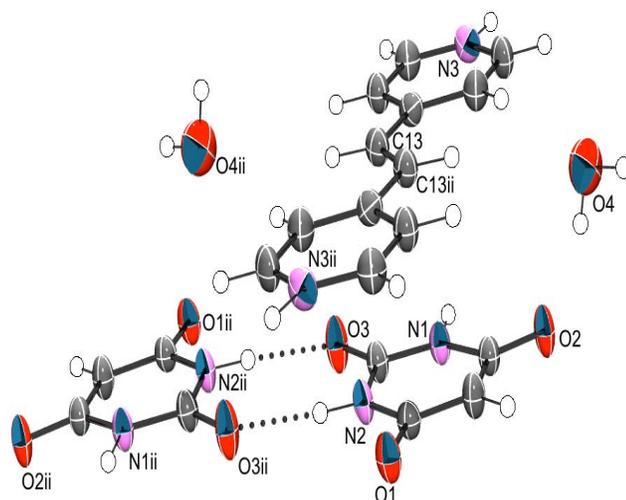
Fig. (2). ORTEP view of the (H$_2$bpe)B$_2$·2H$_2$O (**1**) crystal structure. Ellipsoids are drawn at the 50% probability level except for hydrogen atoms, which are represented by circles of an arbitrary radius. Symmetry code: *(i): x, y, z* and *(ii): -x, -y, -z.*
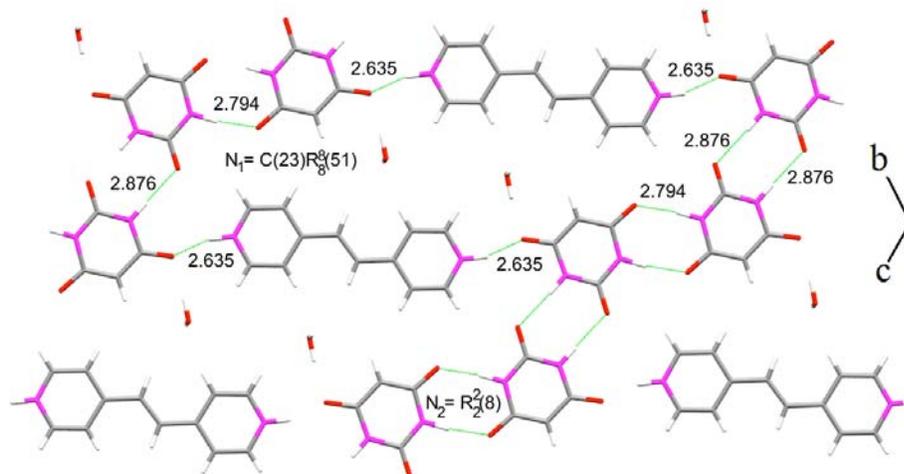
Fig. (3). Bi-dimensional arrangement through hydrogen interactions that were parallel to the *bc* plane for the (H$_2$bpe)B$_2$·2H$_2$O (**1**) complex.

Fig. (**4**) shows the one-dimensional molecular arrangement for compound **2**, which displays the cationic unit and contains the coordinated iron ion sites in a slightly distorted octahedral geometry. The iron sites were formed by four aqua ligands molecules in equatorial positions and two pyridyl nitrogen donors from two different *trans*-1,2-bis(4-pyridil)-ethylene (bpe) ligands in axial positions. The M–O and M–N average bond distances were 2.0978(2) and 2.230(2) Å, respectively, which is comparable to similar distances that have been observed in other compounds [30]. Two uncoordinated barbiturate anions neutralised the structure and interacted through hydrogen bonds, which were classified as moderate to weak due to the interaction distance [24-26]. These moderate to weak hydrogen bonds have O···N distances of 2.804(2) Å (N2···O1) and occur through the NH group of one barbiturate ion (hydrogen donor) and the carbonyl group of the other barbiturate anion (hydrogen acceptor). Completing the repeat unit is the presence of four crystallization crystallisation water molecules, which are omitted from Fig. (**4**) for better visualisation.

Shown in Figs. (**5a** and **5b**) are two representations of the bi-dimensional supramolecular arrangement that is present in compound **2** along the *ac* plane. The supramolecular arrangement was formed by covalent bonds as well as supramolecular interactions, which are the main interactions responsible for the stability of the crystalline arrangement of the system. Fig. (**5a**) shows the molecular arrangement that is constituted by one-dimensional polymeric chains of [Fe(bpe)(H$_2$O)$_4$]$^{2+}$ as the monomeric fragment along the diagonal of the *ac* plane, which generated two different spatial orientations along the *b*-crystallographic axis. The one-dimensional polymer chains did not interact with the neighbouring chains; however, they did interact with the crystallised water molecules that were located in the same plane as the coordination water molecules. Therefore, a two-dimensional array in the *ac* plane was generated by hydrogen bonding. Fig. (**5b**) displays other interactions that were present in the same plane of this structure and were classified as hydrogen bonds between the barbiturate anions and the crystallised water molecules. Along the *a*-crystallographic axis, the barbiturate anions interacted through hydrogen bonds and resulted in a zigzag chain, and the same interactions were present in the *c*-crystallographic axis. The three-
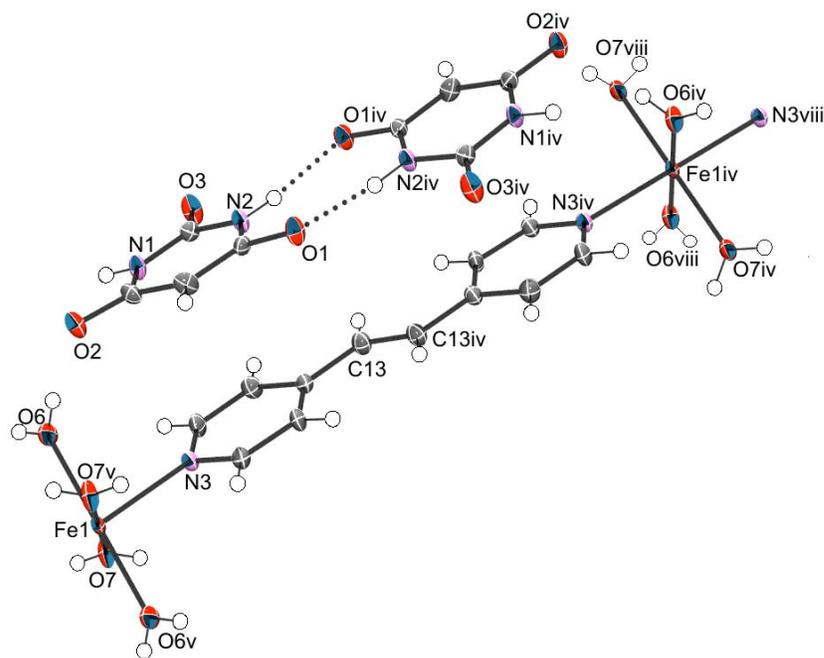
Fig. (4). ORTEP view of the [Fe(bpe)(H$_2$O)$_4$]B$_2$·4H$_2$O (**2**) crystal structure. Ellipsoids are drawn at the 50% probability level except for hydrogen atoms, which are represented by circles of an arbitrary radius. The crystallised water molecules were omitted for clarity. Symmetry code: *(i): x, y, z; (iv): -x+1, y, -z + ½; (v): -x, -y+1, -z; (viii): x + 1, -y + 1, -z + ½.*
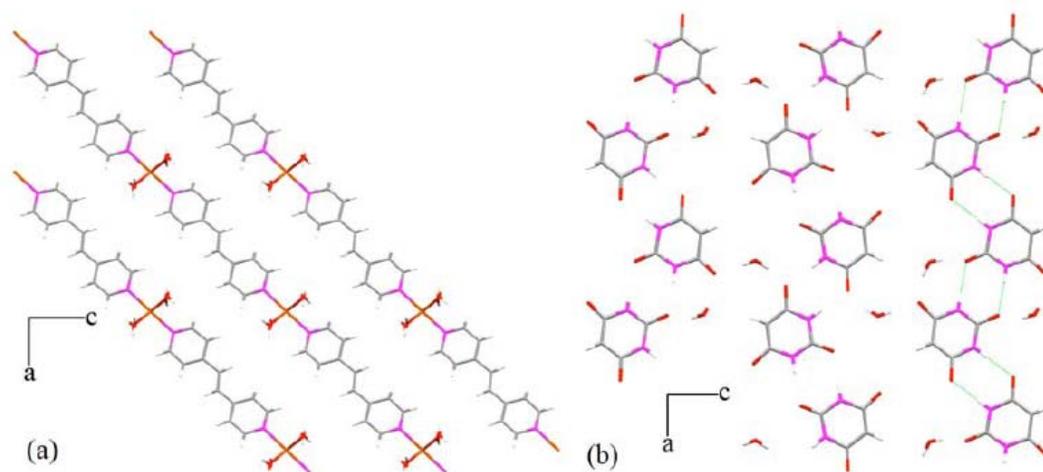
Fig. (5). Formation of two distinct planes of [Fe(bpe)(H$_2$O)$_4$]B$_2$·4H$_2$O (**2**) parallel to the *ac* plane: (**a**) formed covalently through [M(bpe)(H$_2$O)$_4$]$^{2+}$, (**b**) formed by hydrogen interactions between the barbiturate anions and crystallised water molecules.

dimensional arrangement of this structure was observed along the *b*-crystallographic axis with the presence of hydrogen bond interactions between the crystallised water molecules that were located between the layers with the coordination of water molecules and oxygen atoms that were present in the structure of anionic barbiturates. Propagation of these interactions produced rings that are shown in the supplementary material (Figs. **S3** and **S4**). In the *ac* plane, the interaction between barbiturate anions and coordinated and crystallised water molecules produced two types of independent rings that were classified as $N_1 = R_3^3(10)$ and $N_2 = R_3^4(14)$ according to the literature [27, 28]. Another supramolecular interaction that occurred between the rings of the bpe ligand and the anionic barbiturate for compound **2** were the cen-

troid–centroid and interplanar distances that were between 3.53 and 3.45 Å. These results indicated that this compound contained an effective π-stacking interaction.

The vibrational spectra of all ligands and complexes **1** and **2** are shown in Figs. (**6** and **7**) (infrared and Raman spectra, respectively). The main vibrational modes and the respective assignments were based on similar chemical systems and are summarised in Table **3** [31-33]. In both structures, we observed similar vibrational spectra, which include bands that unequivocally confirmed the presence of the bpe ligand and barbiturate anion in the formation of the supramolecular structure.

The barbiturate salt used in the vibrational measurements was synthesised from a reaction between barbituric acid and
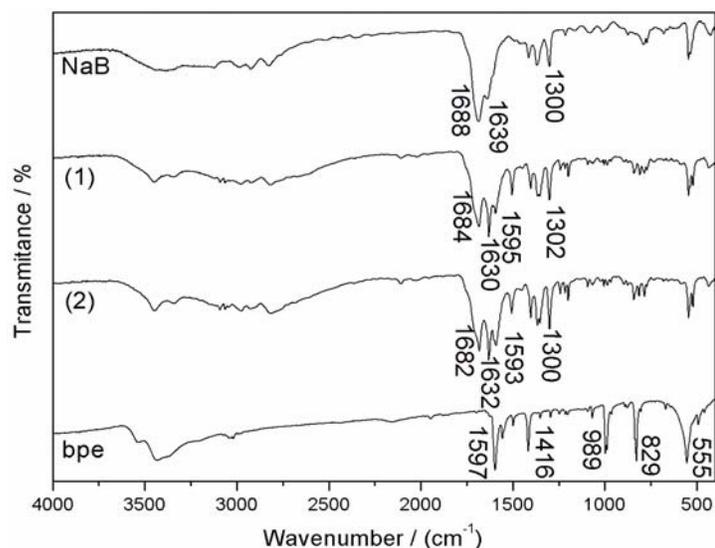
Fig. (6). Infrared spectra of (H$_2$bpe)B$_2$·2H$_2$O (**1**) and [Fe(bpe)(H$_2$O)$_4$]B$_2$·4H$_2$O (**2**); for comparison purposes, the spectra of the ligands (bpe and NaB) are also displayed.
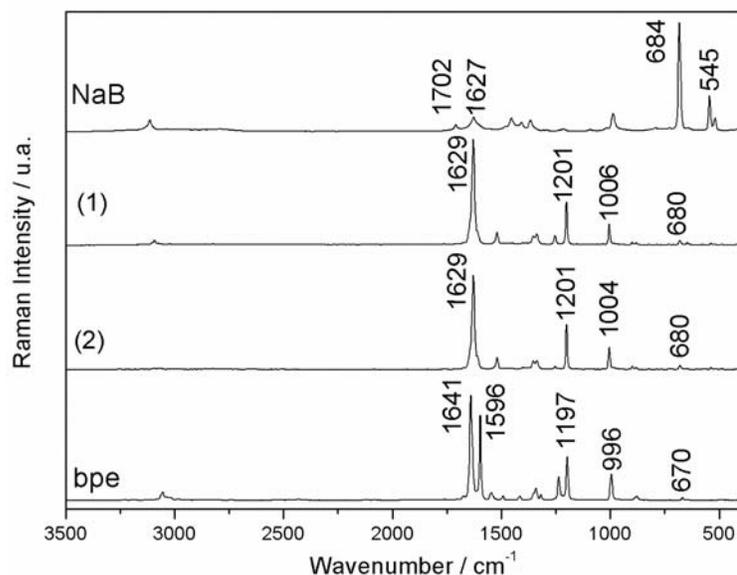
Fig. (7). Raman spectra (excited at 1064 nm) of (H$_2$bpe)B$_2$·2H$_2$O (**1**) and [Fe(bpe)(H$_2$O)$_4$]B$_2$·4H$_2$O (**2**); for comparison purposes, the spectra of the ligands (bpe and NaB) are also displayed.

sodium hydroxide, which formed the dihydrate species and was confirmed by elemental analysis. The infrared spectrum of the barbiturate anion shows a broad band at 3400 cm^{-1}, which was assigned to the OH stretching mode [ν(OH)] and indicated the presence of water molecules in the starting building block. Two other intense modes appeared at 1688 and 1639 cm^{-1}, which were attributed to ν(CO) of the carbonyl groups in different chemical environments (C$_{4,6}$=O and C$_2$=O, respectively, following the numbering of Fig. **1**). According to Barnes *et al*. [34], these vibrations appeared in barbituric acid at 1764 and 1747 cm^{-1}, respectively, which suggests the weakening of the CO bond was caused by the loss of a hydrogen atom from the structure and the formation of several resonance structures to stabilise the system. Three other bands of low intensity were present at 1412, 1369 and 1302 cm^{-1}, which refer to the ν(CN), δ(NH) and combination modes [ν(ring) + γ(CH)], respectively. In the Raman spec-

trum of the barbiturate anion, characteristic modes were observed; for example, the two bands at 1702 and 1627 cm^{-1} were related to the ν(CO) in the structure. Another feature that appeared as an intense band at 680 cm^{-1} referred to the ring-breathing mode. De Oliveira *et al*. [32] investigated the main vibrational modes of barbituric acid by ordinary Raman and SERS (surface-enhanced Raman effect) spectroscopy, and they assigned the bands at 1735 and 1697 cm^{-1} to CO stretching, which was similar to our infrared spectra where these bands were shifted to lower wavenumbers. Another intense band was observed at 665 cm^{-1} and was attributed to the ring-breathing mode. Due to the delocalisation of the electronic charge over the barbiturate anion along the ring (strengthening of the ring bonds), a shift to higher wavenumbers for vibrational modes that involved the ring was expected and was present at 680 cm^{-1}.

Table 3. **Raman (R) and Infrared (IR) Wavenumbers (in cm^{-1}) and Tentative Assignment of the Most Important Bands Observed for the (H$_2$bpe)B$_2$·2H$_2$O (1) and [Fe(bpe)(H$_2$O)$_4$]B$_2$·4H$_2$O (2) Spectra**

NaB		bpe		(H$_2$bpe)B$_2$·2H$_2$O (1)		[Fe(bpe)(H$_2$O)$_4$]B$_2$·4H$_2$O (2)		
IR	**R**	**IR**	**R**	**IR**	**R**	**IR**	**R**	**Tentative Assignment**
		556 vs		544 m		546 m		$\delta_{CH} + \delta_{i.pC\text{-}C}$
	620 w							$\delta_{o.p.\ CO}$
			670 w					Ring breathing
	684 vs				680 w		680 w	Ring breathing
		829 vs						$\delta_{i.p.C\text{-}N} + \nu_{C\text{-}C}$
			879 w					$\delta_{C=C}$
	969 m							ν_{ring}
		989 vs	996 m		1006 m		1004 m	ν_{ring}
		1070 w						$\delta_{CH} + \delta_{i.pC\text{-}C}$
			1197 s		1201 s		1201 s	$\nu_{C\text{-}C}$
1234 m								ν_{CN}
			1237 m					$\delta_{i.pCH}$
1300 m				1302 m		1300 m		$\nu_{ring}+\delta_{o.p\ CH}$
			1342 w					$\delta_{CH} + \nu_{CC}$
1369 w	1367 w			1350 m		1352 m		$\delta_{i.p.NH}$
1412 s				1404 m		1404 m		ν_{CN}
		1416 vs						ν_{CC}
			1492 w	1506 w		1506 m		$\nu_{C\text{-}N} + \nu_{C\text{-}C}$
		1556 s	1548 w					$\nu_{C\text{-}N} + \nu_{C\text{-}C}$
		1596 vs	1596 vs	1595 s	1604 sh	1593 s	1604 sh	ν_{CC} / ν_{CN}
1636 s	1627 w							$\nu_{C2=O}$
		1641 vs		1630 vs	1629 vs	1632 vs	1629 vs	$\nu_{C=Cv}$
1688 vs	1702 w			1684 vs		1682 vs		$\nu_{C4,6=O}$
		3036 w	3054 w					ν_{CH}
	3114 m							ν_{NH}
3400 br								ν_{OH}

Abbreviations: vs, very strong; s, strong; m, medium; w, weak; B, barbiturate anion; i.p., in-plane; o.p., out-of-plane; v,vinyl; br, broad; sh, shoulder.

For the bpe free ligand, the infrared spectrum showed characteristic bands, such as the band at 1597 cm^{-1} that was assigned to νCC/νCN stretching of the pyridyl ring. Two other intense bands were present at 1416 and 989 cm^{-1} and were attributed to the ν(CC) and ν(ring), respectively. The Raman spectrum displayed two intense bands at 1641 and 1596 cm^{-1}, which were assigned to ν(C=C) stretching of the carbon atoms of the aliphatic chain between the pyridyl rings and ν(CC)/ν(CN) of the same ring. For the bpe ligand, the spectral region (for both infrared and Raman spectra) between 1590 and 1650 cm^{-1} where CC and CN stretching modes were important for confirming the coordination or other disturbances caused to the structure, which could be seen through a simple change in position or intensity of the vibrational modes. For the same reasons, the feature at 996 cm^{-1}, which was assigned to the ν(ring) mode, appeared as a low intensity band.

The infrared spectra of compounds **1** and **2** exhibited two broad bands between 3500–3200 cm^{-1}, which were assigned to the ν(OH) and ν(NH) modes of H$_2$O and the NH of the barbiturate anion, respectively. The presence of the broad band at *ca*. 3300 cm^{-1} indicated the hydration of the compounds, which was previously confirmed by thermogravimetric analysis and the structural study of the system. These water molecules were also responsible for the stability of the main supramolecular interactions present in both complexes. Moreover, the presence of the barbiturate anion was determined by the presence of a high intensity band at 1682 cm^{-1}, which was assigned to the ν(CO) mode. Three other bands of low intensity, which appeared at 1404, 1350 and 1302 cm^{-1}, were assigned to the ν(CN), δ(NH) and combination modes [ν(ring) + δ(CH)], respectively. These last three modes assisted in the unequivocal confirmation of the presence of the barbiturate anion in the structure because these

bands were present in a region where bpe has no vibrational activity. Two other intense modes, with one occurring at 1595 cm^{-1} due to $\nu(CC)/\nu(CN)$ stretching and the other at 1630 cm^{-1}, which was due to the $\nu(C=C)$ mode of skeletal chain between the two pyridyl rings, aided in the determination of the presence of the bpe ligand in the structure. The last band appeared to be shifted to a lower wavenumber in both compounds, which suggested a perturbation in compound **1** that was caused by the protonation of the nitrogen atoms of the pyridyl ring and for compound **2**, the coordination of the metallic site to the nitrogen ligand. This band was expected to be present around 1640 cm^{-1} (as observed in the Raman spectrum); however, a loss of electrons caused by protonation and coordination of the nitrogen atom of the pyridyl ring likely caused a weakening of the C=C bond, which was involved in the resonance structure (Fig. **1**). The appearance of this band in the infrared spectrum, which was previously absent in the free ligand measurement, was likely due to a change in the symmetry of the bpe ligand in the formation of compounds **1** and **2**.

Raman spectra of the compounds (Fig. **7**) obtained at 1064 nm excitation wavelengths supported of the observations that were made based on the infrared spectra. The presence of bpe in the structure was confirmed by the observation of the bands at 1629 and 1006 cm^{-1}, which were assigned to the $\nu(C=C)$ and $\nu(ring)$, respectively. These modes appeared to be shifted to lower and higher wavenumbers, respectively, which suggests a process of coordination and protonation of compounds **1** and **2** similar to what was observed in the infrared spectrum. Another band was also observed in both compounds at 1201 cm^{-1} and was assigned to $\nu(C-C)$ mode stretching. The spectra of both complexes shifted to a lower wavenumber for the high intensity bpe band at 1641 cm^{-1}, which was assigned to the C=C stretching mode. In the infrared spectrum, this band was shifted for 1629 cm^{-1}. The presence of the barbiturate anion was observed by a band of low intensity that was located at 680 cm^{-1} and was attributed to ring breathing.

In summary, in this study we have reported the synthesis and results of the spectroscopic (infrared and Raman) and structural investigation of two novel supramolecular compounds, (H$_2$bpe)B$_2$·2H$_2$O (**1**) and [Fe(bpe)(H$_2$O)$_4$]B$_2$·4H$_2$O (**2**), which were obtained from *trans*-1,2-bis(4-pyridyl) ethylene (bpe) and the barbiturate anion for compound **1** and bpe, the barbiturate anion and iron sulphate for compound **2**. For compound **1**, the absence of the metal ion in the formation of the complex was interesting because zinc sulphate was present in the synthesis. The molecular complex shows that the stability of the crystal lattice was due to electrostatic supramolecular interactions between cationic and anionic building blocks, which were formed through an acid/base reaction and the hydrogen bonds between the barbiturate anions and the crystallised water molecules. These noncovalent interactions resulted in the three-dimensional structure, which was responsible for the stability of the crystalline structure. For compound **2**, the presence of the metal in the complex generated a slightly distorted octahedral geometry where the iron ion was coordinated to two pyridine nitrogen atoms from bpe in the axial position and four oxygen atoms from coordinated water molecules in the equatorial positions. All structures contained a covalent linear chain with cationic

monomeric [Fe(bpe)(H$_2$O)$_4$]$^{2+}$ fragments, which were neutralised by two barbiturate anions. The one-dimensional chain interacted with the barbiturate anions and the crystallised water molecules through π-stacking and the hydrogen bonds of the supramolecular interactions, which generated the three-dimensional arrangement where the hydrogen bonds were responsible for the stability of the crystalline array. The vibrational (infrared and Raman) spectra of complexes **1** and **2** were similar, which suggests that protonation and coordination to the nitrogen ligand provided the same type of disturbance for the studied systems. The infrared spectra all contained two intense bands at 1684 and 1630 cm^{-1}, which were assigned to the CO stretching modes of the barbiturate anion and the C=C stretching mode of bpe, respectively. In the Raman spectra, the most important bands were attributed to bpe, such as the bands at 1629 and 1006 cm^{-1}, which were assigned to $\nu(C=C)$ and $\nu(ring)$, respectively. The presence of the barbiturate anion was confirmed by the presence of a band of low intensity that was located at 680 cm^{-1} and was due to ring breathing.

This work demonstrates that the use of multifunctional organic ligands that contain nitrogen atoms and carbonyl groups are very powerful building blocks for the preparation of different supramolecular complexes. Additionally, the use of suitable metallic sites for a particular type of ligand and the prediction of new types of interactions formed are factors that must be patiently studied under the focus of supramolecular chemistry.

SUPPLEMENTARY DATA

Supplementary material is available on the publishers web site along with the published article.

ACKNOWLEDGEMENTS

REFERENCES

[1]   Ruben M, Lehn J-M, Müller P. Addressing metal centres in supramolecular assemblies. Chem Soc Rev 2006; 35: 1056-67.
[2]   Badjc JD, Nelson A, Cantrill SJ, *et al*. Multivalency and cooperativity in supramolecular chemistry. Acc Chem Res 2005; 38: 723-32.
[3]   Jung EJ, Lee U, Koo BK. Synthesis and crystal structure of one-dimensional zinc(II) polymer constructed by salicylate and trans-1,2-bis(4-pyridyl)ethylene. Inorg Chim Acta 2009; 362: 1655-9.
[4]   LaDuca RL. Aliphatic and aromatic carboxylate divalent metal coordination polymers incorporating the kinked and hydrogen-bonding capable tethering ligand 4,4'-dipyridylamine. Coord Chem Rev 2009; 253: 1759-92.
[5]   Zhang Y, Thompson A, Rettig SJ, Dolphin D. The use of dipyrromethene ligands in supramolecular chemistry. J Am Chem Soc 1998; 120: 13537-8.
[6]   Noro S-I, Kitaura R, Kondo M, *et al*. Framework engineering by anions and porous functionalities of Cu(II)/4,4'-bpy coordination polymers. J Am Chem Soc 2002; 124: 2568-83.
[7]   Li XY, Wu YQ, Gu DD, Gan FX. Optical characterization and blu-ray recording properties of metal(II) azo barbituric acid complex films. Mater Sci Eng B 2009; 158: 53-7.
[8]   Li L, Chen B, Song Y, *et al*. Synthesis, crystal structure and third-order nonlinear optical properties of a novel coordination polymer [Cd(en)(NO$_3$)$_2$(4,4'-bpy)]$_n$ containing three kinds of ligands (en = ethylenediamine). Inorg Chim Acta 2003; 344: 95-101.

[9]   Refat MS, El-Korashy SA, Ahmed AS. A convenient method for the preparation of barbituric and thiobarbituric acid transition metal complexes. Spectrhochim Acta A 2008; 71: 1084-94.

[10]   Braga D, Cadoni M, Grepioni F, *et al*. Solid-gas reactions between 1,3-dimethylbarbituric acid and amines. A structural and spectroscopic study. New J Chem 2007; 31: 1935-40.

[11]   Nichol GS, Clegg W. Classical and weak hydrogen bonding interactions between 4,4'-bipyridine and organic acids: from co-crystal to organic complex. Cryst Growth Des 2009; 9: 1844-50.

[12]   Muthiah PT, Hemamalini M, Bocelli G, Cantoni A. Hydrogen-bonded supramolecular motifs in crystal structures of trimethoprim barbiturate monohydrate (I) and 2-amino-4,6-dimethylpyrimidinium barbiturate trihydrate (II). Struct Chem 2007; 18: 171-80.

[13]   Ivanova BB, Spiteller M. Possible application of the organic barbiturates as NLO materials. Cryst Growth Des 2010; 10: 2470-4.

[14]   Garín J, Orduna J, Rupérez JI, *et al*. Second-order nonlinear optical properties of tetrathiafulvanene-π-(thio)barbituric acid chromophores. Tetrahedron Lett 1998; 39: 3577-80.

[15]   Bauer W, Weber B. X-ray structure and magnetic properties of dinuclear and polymer iron(II) complexes. Inorg Chim Acta 2009; 362: 2341-6.

[16]   Pizzotti M, Ugo R, Roberto D, Bruni S. Organometallic counterparts of push-pull aromatic chromophores for nonlinear optics: push-pull heteronuclear bimetallic complexes with pyrazine and trans-1,2-bis(4pyridyl)ethylene as linkers. Organometallics 2002; 21: 5830-40.

[17]   Zou H-H, Yin X-H, Sun X-J, *et al*. A unique 2D framework containing rhombic tetrameric cobalt(II) of mixed T_d and O_h geometries linked by two different rigid ligands: synthesis, crystal structure and magnetic properties. Inorg Chem Commun 2010; 13: 42-5.

[18]   CryAlis RED. Oxford Diffraction Ltd., Version 1.171.32.38 (release 17-11-2008 CrysAlis171. NET) (Compiled Nov 17 2008, 13: 58: 09).

[19]   Sheldrick GM. SHELXL-97 – A Program for Crystal Structure Refinement, University of Goettingen, Germany, 1997.

[20]   Larson AC. The inclusion of secondary extinction in least-squares refinement of crystal structures. Crystallogr Comput 1969; 291-4.

[21]   Blessing RH. An empirical correction for absorption anisotropy. Acta Crystallogr A 1995; 51: 33-8.

[22]   Farrugia LJ. ORTEP-3 for windows-a version of ORTEP-III with a graphical user interface (GUI). J Appl Crystallogr 1997; 30: 565.

[23]   Macrae CF, Edgington PR, McCabe P, *et al*. Mercury: visualization and analysis of crystal structures. J Appl Crystallogr 2006; 39: 453-7.

[24]   Desiraju GR. Hydrogen bridges in crystal engineering: interactions without borders. Acc Chem Res 2002; 35: 565-73.

[25]   Bent HA. Structural chemistry of donor-acceptor interactions. Chem Rev 1968; 68: 587-648.

[26]   Avvaru BS, Kim CU, Sippel KH, *et al*. A short, strong hydrogen bond in the active site of human carbonic anhydrase II. Biochemistry 2010; 49: 249-51.

[27]   Bernstein J, Davis RE, Shimoni L, Chang N-L. Patterns in hydrogen bonding: functionality and graph set analysis in crystals. Angew Chem Int Ed Engl 1995; 34: 1555-73.

[28]   Garcia HC, Diniz R, Yoshida MI, Oliveira LFC. An intriguing hydrogen bond arrangement of polymeric 1d chains of 4,4'-bipyridine coordinated to Co^{2+}, Ni^{2+}, Cu^{2+} and Zn^{2+} ions having barbiturate as counterions in a 3d network. CrystEngComm 2009; 11: 881-8.

[29]   Khlobystov AN, Blake AJ, Champness NR, *et al*. Supramolecular design of one-dimensional coordination polymers based on silver(I) complexes of aromatic nitrogen-donor ligands. Coord Chem Rev 2001; 222: 155-92.

[30]   Garcia HC, Almeida FB, Diniz R, Yoshida MI, Oliveira LFC. Supramolecular structures of metal complexes containing barbiturate and 1,2-bis(4-pyridyl)-ethane. J Coord Chem 2011; 7: 1125-38.

[31]   Garcia HC, Diniz R, Yoshida MI, Oliveira LFC. Synthesis, structural studies and vibrational spectroscopy of Fe^{2+} and Zn^{2+} complexes containing 4,4'-bipyridine and barbiturate anion. J Mol Struct 2010; 978: 79-85.

[32]   Oliveira LFC, Santos PS, Rubim JC. Fourier transform and surface-enhanced Raman spectra of barbituric acid and of its anion. J Raman Spectrosc 1991; 22: 485-8.

[33]   Zhuang Z, Cheng J, Jia H, *et al*. Density functional theory calculation of vibrational spectroscopy of trans-1,2-bis(4-pyridyl)-ethylene. Vib Spectrosc 2007; 43: 306-312.

[34]   Barnes AJ, Legall L, Lauransan J. Vibrational spectra of barbituric acid derivatives in low-temperature matrice. J Mol Struct 1979; 56: 15-27.